Journal of Physics: Conference Series **2462** (2023) 012030 doi:10.1088/1742-6596/2462/1/012030

The Ultra-Slow Muon beamline at J-PARC: present status and future prospects

S Kanda[1,2,3], N Teshima[1,2], T Adachi[4], Y Ikedo[1,2], Y Miyake[1,2,3], Y Nagatani[1,2,3], S Nakamura[5], Y Oishi[1,2,3], K Shimomura[1,2,3], P Strasser[1,2,3], and T Umezawa[5]

[1] Muon Science Laboratory, Institute of Materials Structure Science, High Energy Accelerator Research Organization (KEK), 1-1 Oho, Tsukuba, Ibaraki 305-0801, Japan
[2] Muon Science Section, Materials and Life Science Division, J-PARC Center, 2-4 Shirane Shirakata, Tokai, Naka, Ibaraki 319-1195, Japan
[3] Department of Materials Structure Science, School of High Energy Accelerator Science, The Graduate University of Advanced Studies (SOKENDAI), 1-1 Oho, Tsukuba, Ibaraki 305-0801, Japan
[4] Nishina Center for Accelerator-based Science, RIKEN, Hirosawa-2-1, Wako, Saitama 351-0198, Japan
[5] College of Engineering, Ibaraki University, 4-12-1 Nakanarusawa, Hitachi, Ibaraki 316-8511, Japan

E-mail: `kanda@post.kek.jp`

Abstract. At J-PARC MLF, MUSE provides the world-highest flux of pulsed muon beams. U-Line, one of the four beamlines in the facility, features an intense surface muon beam from Super-Omega and Ultra-slow muon generated by laser ionization of thermal muonium in vacuo. The Ultra-slow muon beam is characterized by variable energy from sub-keV to tens of keV and a time resolution of several tens of times better than that of ordinary pulsed beams. These features enable the study of interesting phenomena localized at surfaces and near interfaces and fast dynamics that cannot be observed with ordinary pulsed beams. Commissioning of the beamline and instruments is underway in preparation for the start of user programs. This paper presents an overview of the facility, its current status, and its prospects.

1. Introduction

Muons play an active role in materials science as microscopic magnetic probes. In accelerator-based experiments, muons are obtained as decay products of pions produced by proton irradiation on a target. In the early days, muons from in-flight decay of pions were used. The energy of decay muons was high, so a large sample was required for a measurement. In 1976, muons produced near the production target surface were found to have a high stopping density in a sample [1]. The beam is so-called the surface muon.

Surface muon beams have been used since the mid-1980s in meson factories. The near-perfect spin polarization, monochromaticity, and high intensity of the beams brought many results in materials science through the muon spin rotation, relaxation, and resonance (μSR) technique. However, their kinetic energy of 4 MeV requires a sufficiently thick sample or a degrader. Therefore, studies of a thin film with surface muon are still difficult.

Investigation of the surfaces and interfaces requires a muon beam with much lower energy than the surface muon. Figure 1 shows the muon implantation depth calculated by a Monte-Carlo simulation using TRIM.SP [2]. Depth-resolved measurements from surface to bulk require energy-tunable monochromatic beams from sub-keV to several tens of keV.

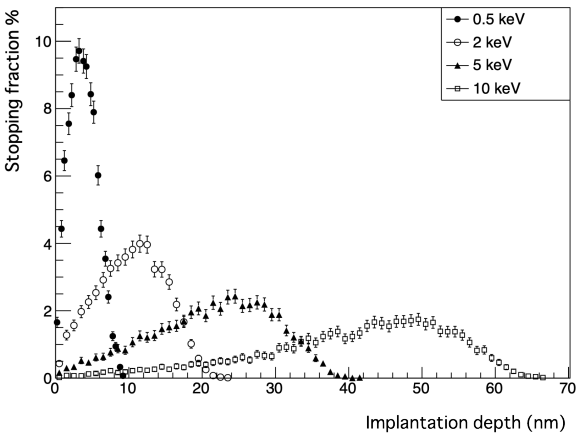

Figure 1. Muon implantation depth profiles in copper calculated by the Monte-Carlo simulation code TRIM.SP. No angular and energy spread of the beam was considered.

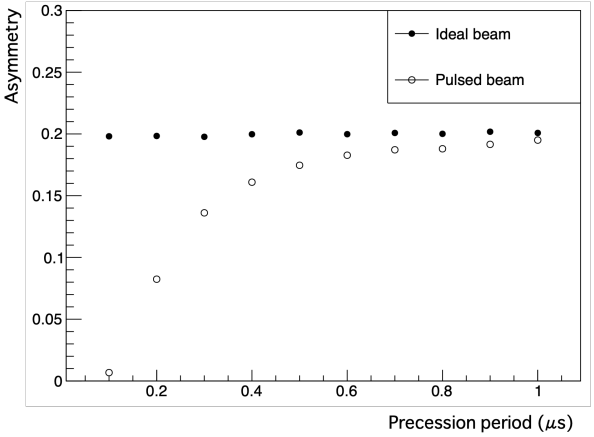

Figure 2. Calculated spin rotation amplitude varying over its period. Solid and open circles indicate the case where the beam has no time width and an FWHM of 100 ns, respectively.

Pulsed muon beams provide high statistics with a good signal-to-noise ratio. However, fast precession is challenging to observe since the time width of pulsed muons dephases the spin rotation. Figure 2 shows the results of a numerical evaluation of the period dependence of amplitude on a simple rotation signal.

A muon beam with variable low energy and short time width extends the application range of μSR to study phenomena at surfaces and interfaces of materials. The Ultra-Slow Muon (USM) obtained by laser ionization of thermal muonium is a unique quantum beam with tunable low-energy and high time resolution.

Using a method for generating low-energy muons based on a different principle than USM, the low-energy muon (LEM) facility at Paul Scherrer Institute (PSI) is under operation [3]. LEM uses a solid rare-gas moderator [4] on a grating substrate [5] to obtain epithermal muons from surface muons. USM and LEM are complementary: USM has superior reachable beam quality in principle, but the current flux is smaller than that of LEM, and the spin polarization is halved due to the use of muonium. On the other hand, LEM uses a continuous beam, which requires a timing counter that spreads beam energy width.

The facility for USM is being commissioned for the start of user programs. In the following sections, we describe the USM generation method, the outline of the facility, the current status, and future plans.

2. Laser ionization of thermal muonium

Muonium is a hydrogen-like atom formed by a positive muon and an electron. It is similar to a hydrogen atom and positronium in some respects but often exhibits different behavior due to differences in mass. This section describes the method of USM generation. Although there are various contexts for thermal muonium production and experiments using it, we will focus here on those directly related to USM at J-PARC.

2.1. Emission of muonium in vacuo

When a positive muon stops in gas or semiconductor, the muon forms muonium. It has been used for muonium spectroscopy and to simulate the behavior of hydrogen atoms in a material. For extraction of USM as a beam, it is necessary to obtain muonium in a vacuum. This is due

to the low energy of USM, which makes transport through the matter difficult.

After several pioneering attempts, thermal muonium emission from current-heated tungsten foil was observed at KEK Booster Meson Facility (BOOM) [6]. The experiment showed that the velocity distribution of emitted muonium follows a Maxwell-Boltzmann distribution. The emission rate was explained as a function of the foil temperature, considering the competition between a decreasing Boltzmann factor and an increasing concentration of lattice defect in the foil. A typical temperature of 2000 K in the experiment corresponds to the kinetic energy of 0.2 eV, which is 5×10^{-8} compared to the energy of surface muons.

2.2. Excitation and ionization of muonium

Muonium in a vacuum moves at a velocity depending on the emitter's temperature. Ionization of thermal muonium yields a low-energy muon with thermal velocity. At KEK BOOM, ionization of thermal muonium with two synchronized laser beams was demonstrated [7]. In the experiment, muonium from hot tungsten was excited to the $2P$ state by laser lights at a wavelength of 122.09 nm and ionized by light at 355 nm. This method of USM generation was taken over and upgraded at the RIKEN muon facility in Rutherford Appleton Laboratory (RAL) [8].

3. The Ultra-Slow Muon beamline at J-PARC MLF MUSE

At J-PARC MLF MUSE [1], the Ultra-Slow Muon beamline consists of a surface muon beam from U-Line, muonium production target, optics for ionization laser, electrostatic lens for extraction, and transport optics. Figure 3 shows a layout of the beamline in the U1 area. The beamline has two branches, U1A for USM-μSR and U1B for transmission muon microscope.

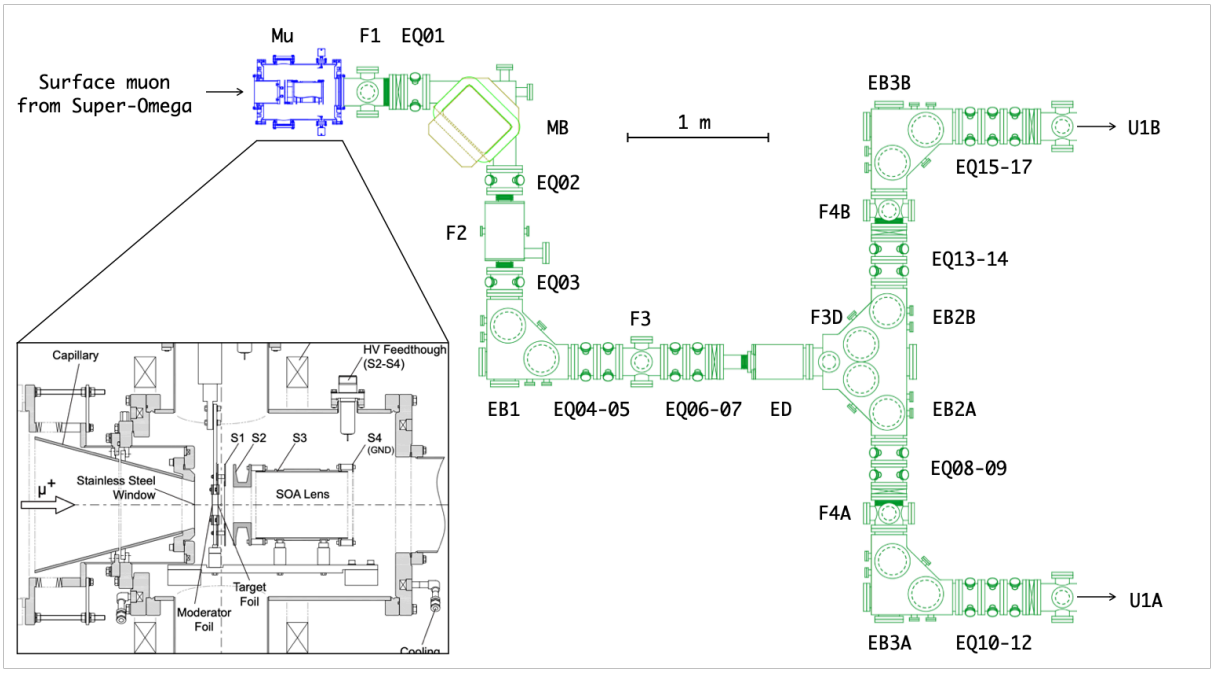

Figure 3. The USM beamline in the U1 area. USMs are obtained by laser ionization of muonium atoms produced at the target (Mu). The transport optics has electrostatic quadrupoles (EQ), a magnetic bend (MB) for momentum selection, electric bends (EB) for energy selection, an electric deflector (ED) for beam destination switching, and detector ports (F). The small inset is a drawing of the muonium target chamber and the extractor taken from the reference [9].

[1] MLF and MUSE stand for Materials and Life Science Facility and Muon Science Establishment, respectively.

3.1. Surface muon beam

The Super-Omega beamline delivers the world's highest flux of pulsed surface muons. The total flux of the beam is on the order of 10^8 μ^+/s. The beamline consists of a large-acceptance capture solenoid [10], a curved solenoid for transport and charge-selection [11], and axial-focusing solenoids with Wien filters [12].

3.2. Muonium production target

As in the KEK BOOM and RIKEN-RAL experiments, a current-heated tungsten foil is used as a muonium emitter. The heating current is pulsed off as the surface muon beam arrives to ensure that the magnetic field generated by the current does not affect the muon spin. The target is heated to 2000 K by applying a current of 430 A. High-temperature tungsten can also be used as an ion source. Lithium ions contained as impurities in the tungsten target were used at U-Line to test and tune the transport optics [13].

3.3. Ionization laser

Thermal muonium is excited to the $2P$ state by 122-nm light (Lyman-α) and ionized by 355-nm light. This scheme is similar to that of KEK BOOM and RIKEN-RAL, but the configuration of the laser system has been sophisticated for better stability and higher ionization efficiency. Details of the system are described in the reference [14].

The typical pulse energy of Lyman-α light reaching the muonium target is approximately 4 to 5 μJ. The width of the laser beam is about 9 mm vertically and 2 mm horizontally. Lyman-α and 355-nm lights are irradiated to muonium atoms almost in parallel and synchronously.

The laser beams should pass as close to the muonium production target as possible while avoiding hitting it. A fluorescent screen and a CMOS camera visualize the beam profiles. The positions and overlap of the laser beams are adjusted by manipulating the steering mirrors inside the vacuum chamber. The laser injection timing is optimized to coincide with the muonium emission time. The trigger timing for laser injection is optimized to maximize the USM yield.

3.4. Extractor

The USMs obtained by laser ionization of muonium are collected while being accelerated by an electrostatic field. An immersion lens developed for positron optics is used for the extraction [15]. The typical extraction energy is 30 keV.

3.5. Transport optics

The configuration of the transport optics is shown in Fig. 3. The energy and momentum of the USM are filtered by electrostatic and magnetic bends (EB and MB), respectively. Electrostatic quadrupole (EQ) lenses are arranged for beam focusing, and a beam profile monitor can be installed at each focusing point (F). The beamline is connected to two experimental areas, and the destination of the beam is selected by switching the polarity of the electrostatic deflector (ED). Characteristics of the transport optics have been studied by a Monte-Carlo simulation considering realistic electric and magnetic field maps [16].

3.6. Beam monitor

The beam profile of the USM is measured by a particle detector based on a microchannel plate (MCP). Because of the large number of background events at the first and second focal points, beam diagnostics are performed primarily at F3 and downstream focus points.

3.7. Muon spin spectrometer

A spectrometer for μSR measurements is located in the U1A experimental area. The spectrometer is entirely on a high-voltage stage to control the USM implantation energy. The detector consists of scintillator blocks connected to silicon photomultipliers (SiPMs) and dedicated front-end electronics. A sample can be installed into the spectrometer without exposure to the atmosphere using a load-lock chamber with a sample transport rod. The sample can be cooled down to 4 K using a helium-flow cryostat, and a longitudinal magnetic field up to 0.14 T can be applied.

4. Present status of the beamline

The beamline is being commissioned for the start of user experiments. This section reports some of the results obtained in FY2021.

4.1. Recent results on the beamline commissioning

In FY2021, the MCP beam monitor at F3 was upgraded from a single anode readout to a delay-line detector (DLD). The MCP-DLD detects the position of a particle from the time difference by reading out both ends of the wires that collect the charge amplified by the MCP. Figure 4 shows a time-of-flight (TOF) spectrum. Typical time width (1σ) of the USM beam is about 2 ns for the high-temperature tungsten at 2000 K. Rapid profile measurements using the MCP-DLD made it possible to optimize various parameters of the transport optics. A result of a two-dimensional scan of the MB currents and the EB1 voltages is shown in Fig. 5.

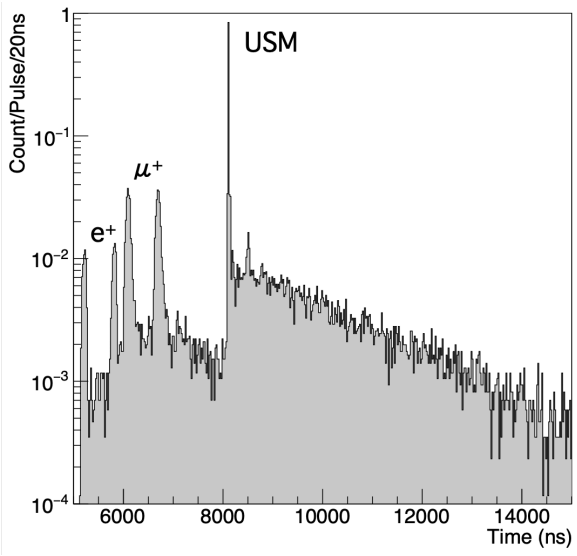

Figure 4. A TOF spectrum measured with the MCP-DLD at F3. The first two peaks correspond to prompt positrons, the next two to muons degraded through the muonium target, and the highest after that to USM.

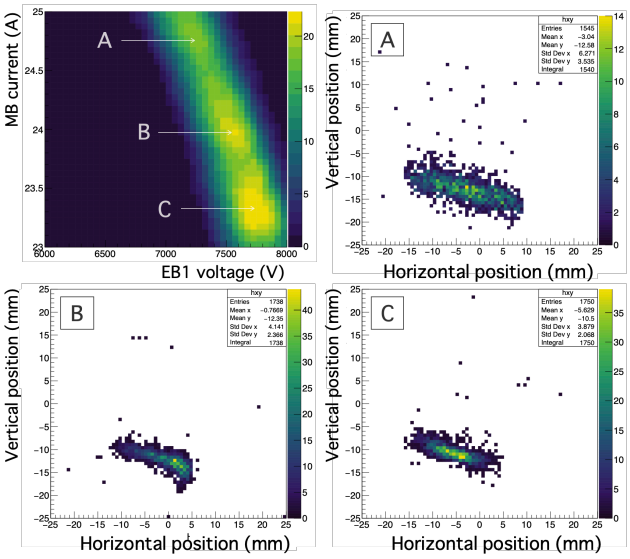

Figure 5. The result of the two-dimensional grid scan of the magnetic and first electric bends. The top left figure shows the yield, and the remaining three give the profile in zones A, B, and C, denoted in the top left.

Figure 5 shows three regions of large yield, each corresponding to a different beam profile. Since a well-focused beam is better suited for smaller samples, it is important to optimize the transport optics not only in terms of yield but also profile.

As a starting point, the transport optics were tuned using the zone C setting shown in Fig. 5. The voltages of the five EQs from EQ01 to EQ05 were changed to search for conditions where

the beam width becomes narrower. The USM beam profile after optimization is shown in Fig. 6. The tuning shaped the beam width to a standard deviation of 1.8 mm (horizontal) and 1.6 mm (vertical). This beam profile is narrow enough compared to typical μSR samples.

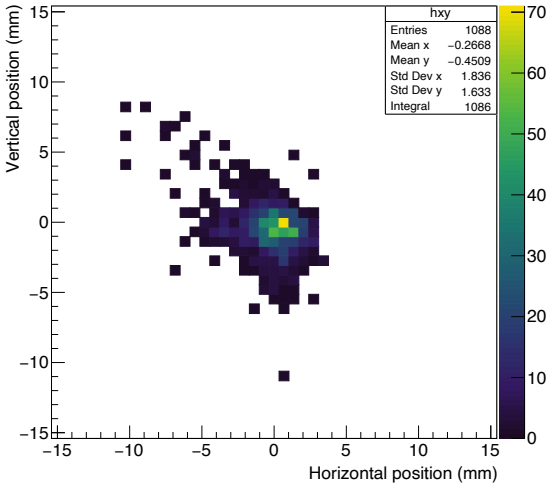

Figure 6. The USM beam profile at F3 after tuning. The beam widths were evaluated by assuming a two-dimensional Gaussian. The horizontal and vertical standard deviations were 1.6 mm and 1.8 mm, respectively.

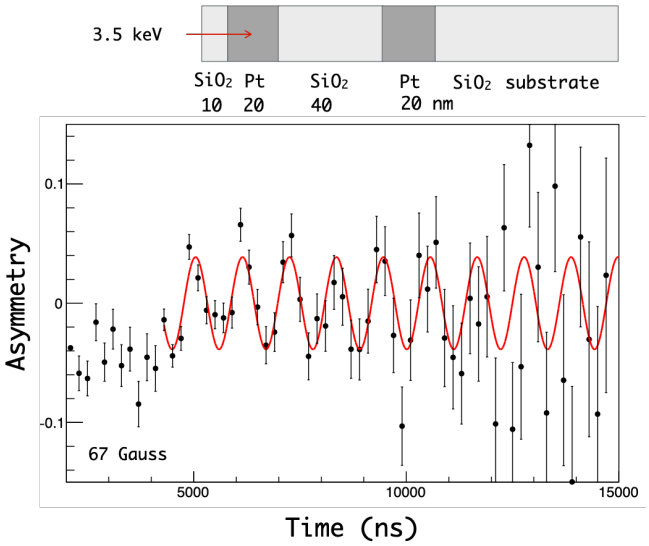

Figure 7. The μSR asymmetry measured by the spectrometer at U1A. USMs at 3.5 keV were implanted into a sample of alternating SiO_2 and platinum layers.

4.2. Feasibility test of USM-μSR

As a feasibility test of μSR measurements, we performed an experiment with a multi-layer sample consisting of alternating layers of SiO_2 and platinum. The energy of USMs was tuned to 3.5 keV to selectively stop muons in the platinum layer sandwiched between the SiO_2 layers. A field of 67 Gauss was applied to observe the muon spin rotation. The positron asymmetry was estimated to be 70% of the full asymmetry obtained with a silver plate [17]. The decrease in asymmetry can be explained by muons also stopping at the adjacent SiO2 layers. For a detailed understanding, an energy scan measurement will be performed.

5. Future prospects

The test experiment conducted in FY2021 showed that USM-μSR is feasible under the present specifications of the USM beam. However, the beam intensity needs to be increased to scan various temperature and magnetic field conditions in a limited beam time allocation. Currently, the USM flux that can be stably delivered is about 300 μ^+/s, and the event rate for a μSR measurement is 60 events/s, taking into account about 20% of the spectrometer's solid angle. This means that it takes about 5 hours to obtain a million statistics. To improve the USM flux, optimization of surface muon transport [18], searching for more efficient muonium emitters, and improving laser pulse energy are being studied. A detailed evaluation of the conversion efficiency of surface muon to USM is also underway.

For surface muon transport, there is room for improvement in focusing and leakage field suppression at the muonium production target. Monte Carlo simulations and beam specification measurements using a semiconductor pixel detector address this issue.

Regarding lasers, the development of a Nd:$Y_3Sc_2Al_3O_12$ (Nd:YSAG) ceramic-based amplifier to improve the pulse energy of Lyman-α light is in progress [14]. A system to monitor the pulse energy and beam profile is being developed to remotely control the optics for stabilization and optimization of the performance.

A systematic study is planned to understand and enhance muonium emission in a vacuum for a muonium production target. As for the spectrometer, a temperature control system with cooling water will be installed to suppress the SiPM gain fluctuation caused by the temperature change due to the heat generated by the magnet. Transverse and zero-field compensation coils are being considered for future upgrades. We also plan to demonstrate the beam polarization control by the spin rotator.

6. Summary

The Ultra-Slow Muon is a powerful probe to investigate the surface and interface in materials with high time resolution. Commissioning of the beamline and spectrometer is underway in preparation for the start of user programs. In the FY2021 commissioning, a method to optimize beam transport conditions using the MCP-DLD was established. A feasibility test with a multi-layer sample demonstrated USM-μSR. The USM flux will be increased by improving surface muon transport, laser pulse energy, and muonium emission efficiency.

Acknowledgements

The authors are very grateful to their colleagues, K. Kawabata, N. Kurosawa, K. Machida, R. Shimizu, and H. Sunagawa, for their contributions to many aspects of the project. We thank Dr. Zaher Salman for the modified version of TRIM.SP with GUI for low-energy muon simulations. One of us (S. K.) would like to thank Dr. Thomas Prokscha, Dr. Xiaojie Ni, and their colleagues at PSI for the support and discussion during his stay at PSI.

References

[1] Pifer A, Bowen T, Kendall K, 1979 *Nucl. Instrum. and Methods* **135** 39
[2] Eckstein W, Computer Simulation of Ion-Solid Interactions, Springer, Berlin, Heidelberg, New York, 1991
[3] E. Morenzoni *et al.*, 2003 *Physica B* **326** 196
[4] E. Morenzoni *et al.*, 1994 *Phys. Rev. Lett.* **72** 2793
[5] T. Prokscha *et al.*, 2001 *Appl. Surf. Sci.* **172** 235
[6] Mills A *et al.*, 1986 *Phys. Rev. Lett.* **56** 1463
[7] Nagamine K *et al.*, 1995 *Phys. Rev. Lett.* **74** 4811
[8] Bakuke P *et al.*, 2008 *Nucl. Instrum. and Methods B* **266** 335
[9] Strasser P *et al.*, 2014 *J. Phys.: Conf. Ser.* **551** 012065
[10] Nakahara K *et al.*, 2009 *Nucl. Instrum. and Methods A* **600** 132
[11] Strasser P *et al.*, 2013 *Nucl. Instrum. and Methods B* **317** 361
[12] Ikedo Y *et al.*, 2013 *Nucl. Instrum. and Methods B* **317** 365
[13] Nagatomo T *et al.*, 2014 *JPS Conf. Proc.* **2** 010102
[14] Oishi Y *et al.*, *J. Phys.: Conf. Ser.* this issue
[15] Canter K F *et al.*, 1986 Modified Soa immersion lens positron gun Positron Studies of Solids, Surfaces and Atoms ed A P Mills Jr et al (Singapore: World Scientific) pp 199-206
[16] Pant A D *et al.*, 2019 *Nucl. Instrum. and Methods A* **929** 129
[17] Adachi T *et al.*, 2018 *KEK-MSL Prog. Rep.* **2018-2** 13.
[18] Teshima N *et al.*, *J. Phys.: Conf. Ser.* this issue